ARTICLE
Journal of Cellular Biochemistry 108:989–997 (2009)

Journal of Cellular Biochemistry

Critical Role of Poly(ADP-Ribose) Polymerase-1 in Modulating the Mode of Cell Death Caused by Continuous Oxidative Stress

Young-Ok Son,[1] Sung-Ho Kook,[2] Yong-Suk Jang,[2,3] Xianglin Shi,[1] and Jeong-Chae Lee[3,4]*

[1] *Graduate Center for Toxicology, University of Kentucky, Lexington, Kentucky 40536-0001*

[2] *Department of Bioactive Material Sciences, Research Center of Bioactive Materials, Chonbuk National University, Jeonju 561-756, South Korea*

[3] *Division of Biological Sciences, Chonbuk National University, Jeonju 561-756, South Korea*

[4] *Institute of Oral Biosciences, 21 Century Education Center for Advanced Public Dental Health (BK 21 Program), Chonbuk National University, Jeonju 561-756, South Korea*

ABSTRACT

Continuously generated hydrogen peroxide (H_2O_2) inhibits typical apoptosis and instead initiates a caspase-independent, apoptosis-inducing factor (AIF)-mediated pyknotic cell death. This may be related to H_2O_2-mediated DNA damage and subsequent ATP depletion, although the exact mechanisms by which the mode of cell death is decided after H_2O_2 exposure are still unclear. Accumulated evidence and our previous data led us to hypothesize that continuously generated H_2O_2, not an H_2O_2 bolus, induces severe DNA damage, signaling poly(ADP-ribose) polymerase-1 (PARP-1) activation, ATP depletion, and eventually caspase-independent cell death. Results from the present study support that H_2O_2 generated continuously by glucose oxidase causes excessive DNA damage and PARP-1 activation. Blockage of PARP-1 by a siRNA transfection or by pharmacological inhibitor resulted in the significant inhibition of ATP depletion, loss of mitochondrial membrane potential, nuclear translocation of AIF and endonuclease G, and eventually conversion to caspase-dependent apoptosis. Overall, the current study demonstrates the different roles of PARP-1 inhibition in modulation of cell death according to the method of H_2O_2 exposure, that is, continuous generation versus a direct addition. J. Cell. Biochem. 108: 989–997, 2009.

KEY WORDS: GLUCOSE OXIDASE; DNA DAMAGE; PARP-1; ATP DEPLETION; MITOCHONDRIAL DEATH EFFECTORS; CASPASES

Numerous studies have focused on investigating the precise mechanisms involved in hydrogen peroxide (H_2O_2)-induced cell death. They have shown that a typical apoptotic process induced by H_2O_2 may involve the condensation and fragmentation of nuclei and the activation of caspase cascades [Barbouti et al., 2002]. However, considerable evidence for H_2O_2 causing non-apoptotic cell death has also been documented. Unlike cells exposed to an H_2O_2 bolus, continuously generated H_2O_2 actually inhibited the execution of the apoptotic process by converting a caspase-dependent to a caspase-independent mode of cell death, where the involvement of apoptosis-inducing factor (AIF) has been proposed [Sancho et al., 2006; Barbouti et al., 2007; Li and Osborne, 2008]. In keeping with this, our previous finding showed that H_2O_2 generated in a low and continuous manner by glucose oxidase induces a caspase-independent, AIF-mediated cell death [Son et al., 2009].

The typical apoptosis process mediated by caspase cascades has energy-requiring steps, and thus a rapid and dramatic reduction of intracellular adenosine triphosphate (ATP) prevents caspase activation and poly(ADP-ribose) polymerase (PARP) cleavage [Cregan et al., 2004; Kang et al., 2004]. A recent observation in our laboratory indicated that an almost complete loss of ATP occurred in cells exposed to H_2O_2 generated by glucose oxidase, not

Abbreviations used: AIF, apoptosis-inducing factor; ATP, adenosine triphosphate; DAPI, 4′-6-diamidino-2-phenylindole; DiOC6, 3,3′-dihexyloxa-carbocyanine iodide; EndoG, endonuclease G; 4HQ, 4-hydroxyquinazoline; MMP, mitochondrial membrane potential; MTT, 3-(4,5-dimethylthiazol-2yl-)-2,5-diphenyl tetrazolium bromide; PARP, poly(ADP-ribose) polymerase; PI, propidium iodide; ROS, reactive oxygen species; SDH, succinate dehydrogenase; SSB, single-strand breaks.

Grant sponsor: KOSEF, Republic of Korea; Grant number: 2009-0067712.

*Correspondence to: Jeong-Chae Lee, Research Center of Bioactive Materials, Institute of Oral Biosciences, Chonbuk National University, Jeonju 561-756, South Korea. E-mail: leejc88@chonbuk.ac.kr

Received 10 July 2009; Accepted 31 July 2009 • DOI 10.1002/jcb.22332 • © 2009 Wiley-Liss, Inc.
Published online 26 August 2009 in Wiley InterScience (www.interscience.wiley.com).

by an H_2O_2 bolus, within 12 h of the exposure [Son et al., 2009]. Although the exact mechanism by which the continuous presence of H_2O_2 induces energy failure is unclear, considerable evidence has emphasized the involvement of PARP-1 [Szabó et al., 1996; Park et al., 2005]. This was also partially supported by the previous finding that a PARP-1 inhibitor, 3′-aminobenzamide, increased DNA fragmentation in glucose oxidase-exposed cells [Son et al., 2009].

PARP-1 is a well-known nuclear enzyme which participates in DNA repair and cell death [Szabó et al., 1996; Bernstein et al., 2002; Erdélyi et al., 2005; Park et al., 2005]. Indeed, over-activation of PARP-1 in response to excessive DNA damage by reactive oxygen species (ROS) or damaging agents rapidly depletes intracellular ATP [Lin and Yang, 2008]. Moreover, the kinetics of DNA damage are more persistent and prolonged under the continuous presence of H_2O_2 as opposed to an H_2O_2 bolus [Barbouti et al., 2002, 2007]. These reports strongly suggest that H_2O_2-mediated change to a caspase-independent cell death is closely related to severe DNA damage and subsequent PARP-1 activation and ATP depletion. However, the precise effects of PARP inhibition in deciding the mode of cell death caused by continuous exposure to H_2O_2 were not explored.

Here we wanted to further examine the role of PARP-1 in regulating cell death induced by continuously generated H_2O_2 versus by a bolus addition of H_2O_2. This study confirms that PARP-1 is the most critical modulator in deciding the type of cell death in H_2O_2-exposed cells, and this is differently affected according to the method of H_2O_2 exposure.

MATERIALS AND METHODS

CHEMICALS

Unless otherwise specified, all chemicals were purchased from Sigma Chemical Co. (St. Louis, MO). All reagents used were prepared immediately before use.

CELL CULTURE AND TREATMENT

BJAB cells were cultured in RPMI-1640 medium supplemented with antibiotics (Gibco™, Grand Island, NY) and 10% fetal bovine serum (FBS; HyClone, Logan, UT). When the cells had reached to confluence, the cells (1×10^6 cells/ml) were divided into 6-well or 96-multiwell plates with 2 and 0.2 ml per well, respectively, in a fresh RPMI-1640 medium supplemented with 0.5% FBS and 5 mM glucose. After 2 h incubation, the cells were exposed to glucose oxidase (0–10 mU/ml) in the presence and absence of 50 μM 4-hydroxyquinazoline (4HQ). In this case, this enzyme (10 mU/ml) generates 1–2.4 μM H_2O_2/min up to 24 h depending on the incubation times [Lee et al., 2006]. Cells were also exposed to 200 μM H_2O_2 by a direct addition of bolus H_2O_2, and if not otherwise specified, an excess of catalase was added into the cultures 3 h after the bolus exposure. At the various times of H_2O_2 exposure, cells were processed for further analyses.

SINGLE-CELL GEL ELECTROPHORESIS (COMET ASSAY)

A comet assay was performed according to the methods described previously with slight modifications [Panayiotidis et al., 1999]. Briefly, H_2O_2-exposed cells were suspended in 1% low melting point agarose in PBS (pH 7.4) and divided onto glass microscope slides. The slides were immersed in a lysis solution at 4°C for 1 h, placed in single rows in an electrophoresis tank, and then electrophoresed at 30 V (1 V/cm) and 300 mA for 30 min. Finally, the slides were washed with 0.4 M Tris (pH 7.5) at 4°C before being stained with ethidium bromide. In addition, the single-strand breaks (SSB) formation after comet assay was placed into five classes (classes 0–4) and the score for 100 comets per each experiment was represented as the DNA damage index as described elsewhere [Panayiotidis et al., 1999; Martin et al., 2002].

MEASUREMENT OF CYTOTOXICITY AND SUCCINATE DEHYDROGENASE (SDH) ACTIVITY

Aliquots of cells were stained with 0.4% trypan blue and approximately 100 cells were counted for each treatment. Cell death was calculated as follows: % cytotoxicity = [(total cells − viable cells)/total cells] × 100%. In addition, 3-(4,5-dimethylthiazol-2yl-)-2,5-diphenyl tetrazolium bromide (MTT) was used to evaluate the SDH activity of cells as described elsewhere [Son et al., 2009].

MEASUREMENT OF MITOCHONDRIAL MEMBRANE POTENTIAL (MMP)

H_2O_2-exposed cells (2×10^6 cells) were stained with 50 nM 3,3′-dihexyloxa-carbocyanine iodide ($DiOC_6$; Molecular Probes, Eugene, OR) for 20 min at 37°C. The fluorescence related to MMP was measured using a FACS Calibur® system (Becton Dickinson, San Jose, CA), and the level of MMP was determined using the WinMDI 2.9 program.

PROPIDIUM IODIDE (PI) STAINING AND CELL-CYCLE ANALYSIS

H_2O_2-exposed cells (2×10^6 cells) were fixed with 70% ethanol at 4°C for 24 h and then incubated at room temperature for 1 h in a staining mixture (1 ml) containing 250 μl of PBS, 250 μl of 1 mg/ml RNase, and 500 μl of 50 μg/ml PI. In each experiment, 10,000 cells were counted to measure PI intensity using a FACS Calibur® system (Becton Dickinson) and the cell-cycle progression was determined using the WinMDI 2.9 program.

AGAROSE GEL ELECTROPHORESIS

After H_2O_2 exposure, BJAB cells were collected and incubated with a lysis buffer [1% nonidet P (NP)-40 and 1% sodium dodecyl sulfate (SDS) in 50 mM Tris, pH 8.0] at 65°C for 1 h. DNA was extracted with phenol/chloroform/isoamyl alcohol, and the formation of DNA ladders was analyzed using 2% agarose gel electrophoresis, followed by ethidium bromide staining.

ATP ASSAY

Intracellular ATP levels were determined using Molecular Probes' ATP determination kit (A22066). Briefly, H_2O_2-exposed cells (2×10^6 cells/ml) were resuspended in a buffer (250 μl) containing 10 mM KH_2PO_4 and 4 mM $MgSO_4$ (pH 7.4) before heating at 98°C for 4 min. ATP levels were determined by using luciferase and its substrate D-luciferin. Finally, light emission was quantified in a MicroLumat Plus LB 964 (Berthold Technologies, Germany).

MEASUREMENT OF CASPASE ACTIVITIES

At various time points (0–24 h) during H_2O_2 exposure, cells were collected and resuspended in a lysis buffer. The lysates (100 μg) were incubated with 100 μM of the synthetic substrate Ac-DEVD-AMC (for caspase-3 activity) or Ac-LEHD-AFC (for caspase-9 activity) at 37°C for 2 h in a reaction buffer (1 ml) containing 100 mM HEPES (pH 7.5), 10% sucrose, 0.1% CHAPS, and 10 mM dithiothreitol (DTT). Fluorescence intensities were measured using a microplate spectrophotometer (Bio-Tek Ins., Vermont, USA).

FLUORESCENCE STAINING

Initially, H_2O_2-exposed cells were fixed with 4% buffered formaldehyde (pH 7.4) at 4°C for 15 min and then stained with 1 μg/ml of Hoechst 33342 at 4°C for 1 h. After washing with DPBS, approximately 200 nuclei from each sample were observed by fluorescence microscopy (Axioskop 2, Carl Zeiss, Germany) and the results were represented as the percentage of normal, condensed, or fragmented nuclei, according to the morphological classification. In addition, the cells were double-stained with Hoechst 33342 (1 μg/ml) and PI (0.5 μg/ml) without chemical fixation. Approximately 200 cells per sample were counted using fluorescence microscopy and classified as follows: (i) non-apoptotic viable cells (normal nuclei, blue chromatin with organized structure); (ii) apoptotic cells (bright blue and/or red chromatin, condensed and fragmented); (iii) pyknotic/necrotic cells (bright blue and/or red, condensed only); and (iv) necrotic cells (red and enlarged nuclei).

WESTERN BLOT ANALYSIS

Protein lysates were made in a lysis buffer as described elsewhere [Son et al., 2009] and the protein content was quantified according to the Bradford method [1976]. Equal protein amounts (30 μg) for each sample were separated by 12% SDS–PAGE and blotted onto PVDF membranes. The blots were probed with primary and secondary antibodies and were then developed with enhanced chemiluminescence (Amersham Pharmacia Biotech, Buckinghamshire, UK) immediately before exposure to X-ray film (Eastman-Kodak, Rochester, NY). Monoclonal antibody against α-tubulin and polyclonal antibody against PAR (528815) were purchased from BD Bioscience Pharmingen (San Diego, CA) and Calbiochem (San Diego, USA), respectively. Unless otherwise specified, other antibodies were obtained from Santa Cruz Biotechnology (Santa Cruz, CA).

IMMUNOFLUORESCENCE ASSAY

After the processes of cell fixation, the cells were incubated with primary antibody specific to AIF or endonuclease G (EndoG) in blocking solution for 2 h prior to staining with FITC-conjugated secondary antibody. Cells were counterstained in a blocking solution containing 1 μg/ml 4′-6-diamidino-2-phenylindole (DAPI) or 0.5 μg/ml PI for 15 min. After being washed three times with PBS, the coverslips were mounted onto microscopic slides and observed under a fluorescence microscope (Axioskop 2).

SMALL INTERFERING RNA TRANSFECTION

Small interfering RNA (siRNA)-mediated silencing of the PARP-1 gene was performed using 21-bp (including a 2-deoxynucleotide overhang) siRNA duplexes purchased from Ambion (Austin, TX). The coding strand for PARP-1 siRNA was 5′-GGC CAG GAU GGA AUU GGU AdTdT-3′. An unrelated siRNA that targeted the green fluorescent protein DNA sequence (5′-CCA CTA CCT GAG CAC CCA GdTdT-3′) was used as a control. In this experiment, cells were put into six-well plates, incubated for 12 h, and transfected at approximately 30% confluency with siRNA duplexes using Lipofectamine 2000 (Invitrogen, Carlsbad, CA) according to the manufacturer's instructions. All the experiments were performed 48 h after transfection.

PREPARATION OF CELL FRACTIONS

Nuclear proteins were prepared as described elsewhere [Maulik et al., 1998] and quantified according to the Bradford method. In addition, H_2O_2-exposed cells were incubated in 150 μl lysis buffer (250 mM sucrose, 20 mM HEPES, pH 7.5, 10 mM KCl, 1.5 mM $MgCl_2$, 1 mM EGTA, 1 mM EDTA, 1 mM DTT, 1 mM PMSF, 10 μg/ml each of leupeptin, aprotinin, and pepstatin A) on ice for 30 min. The cells were centrifuged at 750*g* for 10 min at 4°C, and the supernatants were further centrifuged at 10,000*g* for 25 min at 4°C in order to prepare the cytosolic fraction. The remaining pellets were resuspended in the lysis buffer and used as the mitochondrial fraction after centrifugation at 10,000*g* for 25 min.

STATISTICAL ANALYSIS

All data are expressed as mean ± standard deviation (SD). One-way analysis of variance (ANOVA; SPSS version 16.0 software) followed by Scheffe's test was applied to determine the significant differences between the groups. A *P*-value of <0.05 was considered significant.

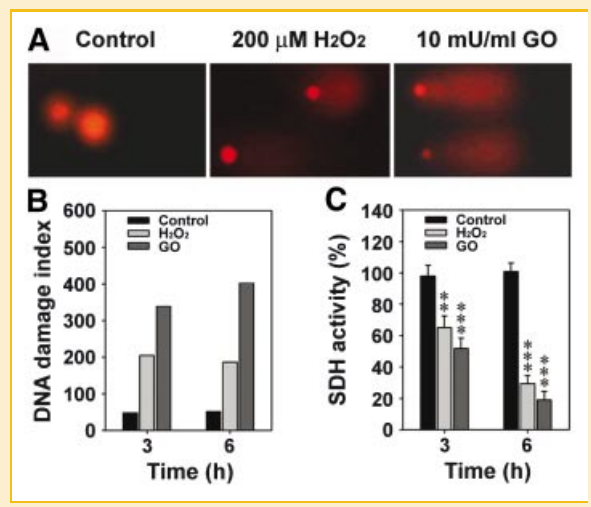

Fig. 1. Effects of H_2O_2 on DNA damage and SDH activity. BJAB cells were exposed to 200 μM H_2O_2 or 10 mU/ml glucose oxidase (GO). A: At the 3 h exposure time point, the cells were embedded in agarose and electrophoresed according to the comet assay. Photographs show a representative result of ethidium bromide–stained nuclei from three independent experiments. B: More than 200 comets/treatment were sorted into five classes, and the DNA damage index was calculated and referred to 100 comets. C: Cells were processed for SDH activity analysis at the indicated H_2O_2 exposure times. $^{**}P<0.01$ and $^{***}P<0.001$ versus the control values. [Color figure can be viewed in the online issue, which is available at www.interscience.wiley.com.]

RESULTS

FORMATION OF SSB WAS MORE PROMINENT IN CELLS EXPOSED TO GLUCOSE OXIDASE THAN TO AN H_2O_2 BOLUS

Consistent with the previous finding [Barbouti et al., 2002], the present data show that the kinetics of DNA damage differ according to the mode of H_2O_2 exposure. More dramatic SSB formation occurred in cells exposed to 10 mU/ml glucose oxidase than a bolus of 200 μM H_2O_2 (Fig. 1A,B). Unlike the results from the comet assay, the data from the MTT assay revealed that SDH activity was inhibited in a time-dependent manner under either exposure scheme (glucose oxidase or H_2O_2 bolus; Fig. 1C). This indicates that H_2O_2 causes mitochondrial stress regardless of the method of H_2O_2 exposure, and that the drop of SDH activity is not associated directly with the DNA damage in H_2O_2-exposed cells.

PARP-1 ACTIVATION IS ASSOCIATED WITH H_2O_2-INDUCED MMP LOSS, CYTOTOXICITY, AND AIF TRANSLOCATION

Exposure of the cells to 10 mU/ml glucose oxidase resulted in a rapid and efficient activation of PARP-1 (Fig. 2A). Blockage of PARP-1 by transfecting with its specific siRNA inhibited its cellular expression (Fig. 2B) and PAR formation (Fig. 2C). The inhibition of PARP-1 by a gene-specific siRNA or by a pharmacological inhibitor, 4HQ (50 μM), significantly attenuated the H_2O_2-mediated loss of MMP (Fig. 2D) and cytotoxicity (Fig. 2E) in cells exposed to 10 mU/ml glucose oxidase for 12 h. However, these protective effects on MMP loss and cell death by blocking PARP-1 were not observed at the 24 h time point (data not shown). Exposure of cells to an H_2O_2 bolus triggered PARP-1 activation only at early time points (around 60 min), and PARP-1 inhibitor did not significantly affect the MMP loss and cytotoxicity caused by adding the H_2O_2 bolus (results not shown). Confocal microscopy analysis of glucose

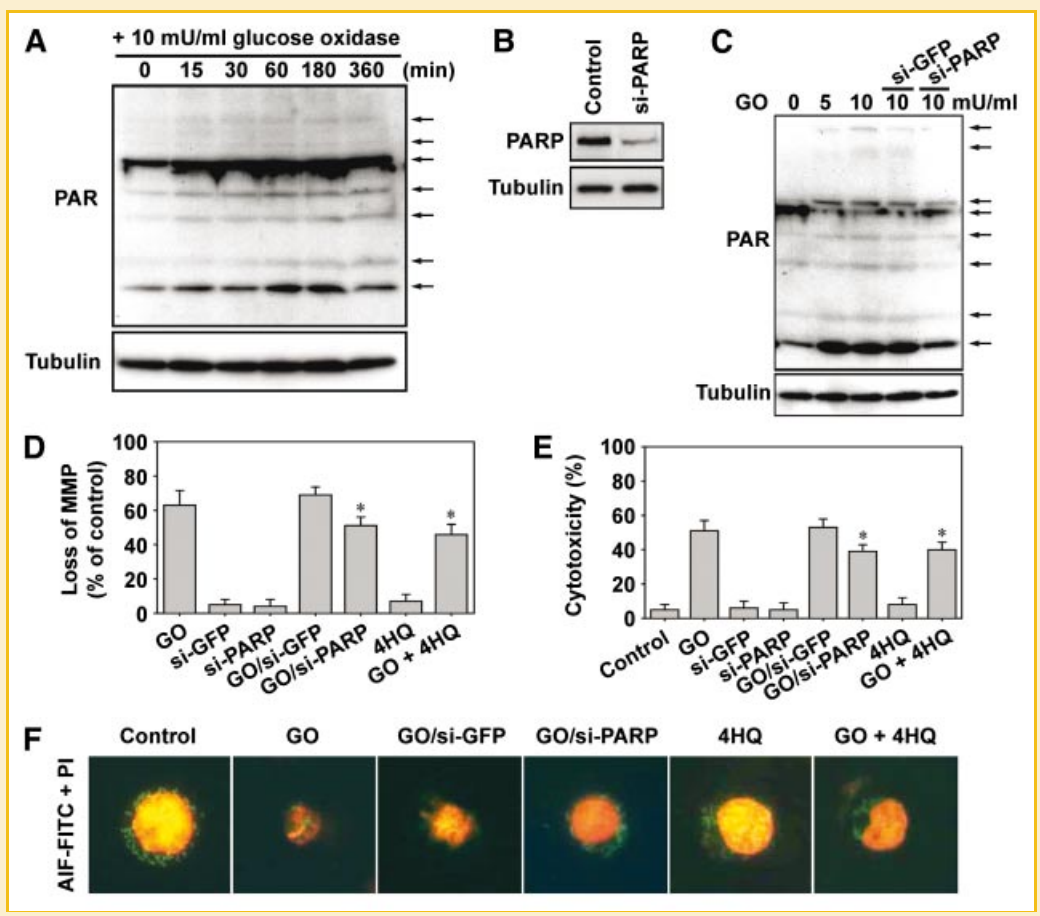

Fig. 2. PARP-1 activation is required for H_2O_2-induced MMP loss, cytotoxicity, and AIF translocation. A: Western blot analysis of PARP-1 activation in cells exposed to 10 mU/ml glucose oxidase for the indicated times. Arrows represent the PAR polymers formed. B: Western blot analysis of cellular PARP-1 levels 18 h after siRNA transfection. C: The GFP or PARP-1-transfected cells (2×10^6 cells) were incubated in the presence or absence of glucose oxidase for 3 h and then PARP-1 activation was analyzed by Western blotting. In addition, control and transfected cells were exposed to 10 mU/ml glucose oxidase with and without 50 μM 4HQ for 12 h and they were then adjusted to determine the levels of MMP (D), cytotoxicity (E), and AIF nuclear translocation (F). $^*P < 0.05$ versus the values of glucose oxidase treatment alone. F: Cells were stained with FITC-AIF and then counterstained with PI prior to analysis by confocal microscope. A representative result from three independent experiments is shown and the overlay represents the fusion image of green (AIF) and red (nucleus). [Color figure can be viewed in the online issue, which is available at www.interscience.wiley.com.]

oxidase-treated cells showed profound inhibition of AIF nuclear translocation and nuclear condensation by blocking PARP-1 activation (Fig. 2F).

PARP-1 ACTIVATION INDUCES ATP DEPLETION IN H_2O_2-EXPOSED CELLS

Blockage of the mitochondrial ATP-generating system leads to caspase-independent apoptosis, in which the genomic DNA ladders and the activation of caspase cascades are not observed [Comelli et al., 2009]. The present study showed that cells exposed to continuously generated H_2O_2 induced severe depletion of intracellular ATP in a time-dependent manner, whereas no dramatic and time-dependent decreases of ATP levels were observed in cells exposed to a bolus of 200 μM H_2O_2 (Fig. 3A). ATP depletion in glucose oxidase-treated cells was blocked by inhibiting PARP-1 activation with its specific siRNA transfection or its pharmacological inhibitor, 4HQ (Fig. 3B). Similarly, another PARP-1 inhibitor, 3′-aminobenzamide, also inhibited ATP reduction in the glucose oxidase-exposed cells but not in the bolus H_2O_2-applied cells (data not shown). However, the SDH activity, which decreased almost completely with either type of H_2O_2 exposure, was not affected by PARP-1 inhibition (Fig. 3C). This means that the mitochondria activity is reduced by H_2O_2 regardless of the method of exposure to this agent.

INHIBITION OF PARP-1 LEADS TO THE EXECUTION OF TYPICAL APOPTOTIC PROCESS IN GLUCOSE OXIDASE-TREATED CELLS

To ensure whether the blockage of PARP-1 ameliorates directly H_2O_2-mediated cytotoxicity or converts only the mode of cell death, we carried out various apoptosis assays. Treatment of cells with 10 mU/ml glucose oxidase for 24 h induced marked cell shrinkage, and this was not affected by combination with 50 μM 4HQ (Fig. 4A). Chromatin staining with Hoechst 33342 showed that glucose oxidase induces nuclear condensation without DNA fragmentation, whereas pretreatment of cells with 50 μM 4HQ significantly increased the number of nuclei with condensed and fragmented in cells exposed to 10 mU/ml glucose oxidase for 24 h (Fig. 4B). Glucose oxidase also induced cell death without a significant increase of population in the sub-G_1 phase of cell-cycle progression, that is, apoptotic cells (Fig. 4C). In contrast, cell population in the sub-G_1 phase was increased in the presence of 4HQ, such that approximately 33% of cells migrated into sub-G_1 phase during co-incubation with 10 mU/ml glucose oxidase and 50 μM 4HQ for 24 h, as compared to only 11% in glucose oxidase alone (Fig. 4C,D). Cells exposed to a bolus H_2O_2 had an apparent increase in the migration of cells into the sub-G_1 phase, which was not augmented by the 4HQ treatment. Agarose gel electrophoresis shows that adding 4HQ into the glucose oxidase-treated cells led to the formation of DNA ladders in glucose oxidase-exposed cells, like those shown in the H_2O_2 bolus-treated cells (Fig. 4E). However, DNA laddering caused by an H_2O_2 bolus was clearly diminished when cells were incubated in combination with glucose oxidase.

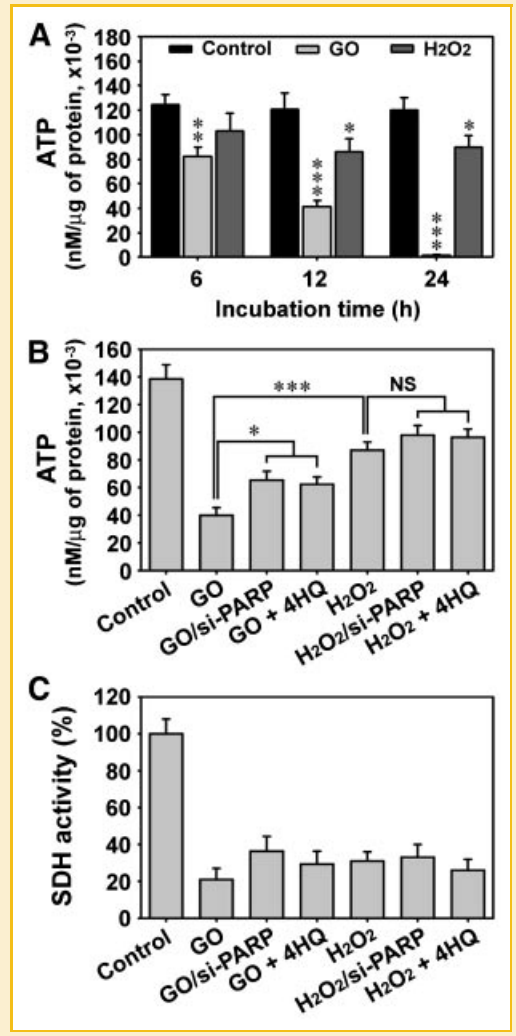

Fig. 3. ATP depletion is blocked by the inhibition of PARP-1 in H_2O_2-exposed cells. A: Cells were exposed to H_2O_2 generated by 10 mU/ml glucose oxidase or to 200 μM H_2O_2 added in bolus form, and then processed for ATP determination. $^{*}P < 0.05$, $^{**}P < 0.01$, and $^{***}P < 0.001$ versus the control values. Control and si-PARP-1-transfected cells were also exposed to the H_2O_2 generating system in the presence and absence of 50 μM 4HQ for 12 h and then processed for determination of ATP level (B) and SDH activity (C). Results show the mean ± SD from three independent experiments, and $^{*}P < 0.05$ and $^{***}P < 0.001$ represent significant differences between the experiments. NS, not significant.

INHIBITION OF PARP-1 SWITCHES CASPASE-INDEPENDENT PYKNOSIS TO CASPASE-DEPENDENT APOPTOSIS IN GLUCOSE OXIDASE-TREATED CELLS

The addition of 10 mU/ml glucose oxidase did not lead to any prominent cleavage of either procaspase-3, procaspase-7, or PARP, as expected (Fig. 5A). Pretreatment with 50 μM 4HQ led to the appearance of bands corresponding to active caspase-3 and intermediate form of caspase-7 with molecular weight of around 20 and 35 kDa, respectively, as well as a cleaved 85 kDa PARP protein in glucose oxidase-treated cells. Such results were similar to results from cells exposed to a 200 μM H_2O_2 bolus.

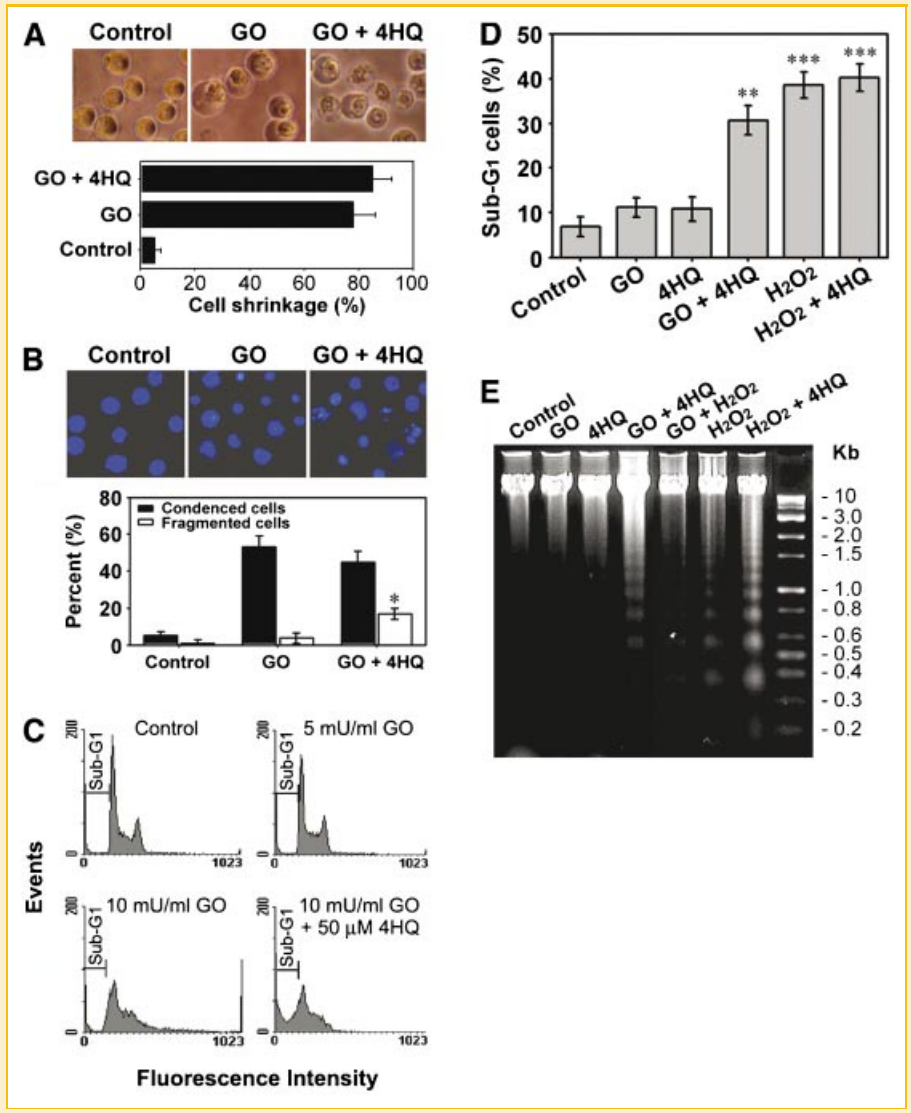

Fig. 4. Inhibition of PARP-1 leads to the execution of typical apoptotic process in glucose oxidase-treated cells. Cells were exposed to 10 mU/ml glucose oxidase or 200 μM H_2O_2 in the presence and absence of 50 μM 4HQ. At the 24th hour of exposure, these cells were processed to observe cell shrinkage (A), chromatin staining with Hoechst 33342 (B), flow cytometric analysis after PI staining (C,D), or agarose gel electrophoresis for DNA laddering observation (E). All experiments were performed at least three times and a representative photograph is shown. For quantitative assessment of cellular and nuclear morphology, more than 200 cells were counted in each sample. The percentage (%) of cell population in sub-G_1 phase, that is, apoptotic cells, was calculated using the WinMDI 2.9 program from three independent flow cytometric data. $^{*}P < 0.05$, $^{**}P < 0.01$, and $^{***}P < 0.001$ versus glucose oxidase treatment alone. [Color figure can be viewed in the online issue, which is available at www.interscience.wiley.com.]

However, co-treatment of cells with glucose oxidase and the H_2O_2 bolus diminished the band intensities corresponding to the active caspases and cleaved PARP that were apparently induced by H_2O_2 bolus. This was confirmed by examining the combined treatment of glucose oxidase and 4HQ, which significantly increased caspase-3-like and caspase-9 activities (Fig. 5B,C). In parallel with these results, caspase activation in glucose oxidase-exposed cells was also observed when they were incubated with 3′-aminobenzamide or when the PARP-transfected cells were examined (data not shown).

Photographs after Hoechst/PI double staining (Fig. 5D) and their quantitative results (Fig. 5E) revealed that treatment of cells with 10 mU/ml glucose oxidase alone mostly induced chromatin condensation, whereas co-treatment with 50 μM 4HQ apparently increased the number of cells representing condensed and fragmented nuclei. Exposure of cells to continuously generated H_2O_2 markedly prevented the apoptotic process induced by adding an H_2O_2 bolus. Inhibition of PARP-1 by 4HQ did not affect the glucose oxidase-mediated DNA damage, whereas antioxidant enzyme catalase (200 U/ml) completely blocked the DNA damage (Fig. 5F). Catalase also markedly inhibited PARP-1 activation induced by the continuous presence of H_2O_2 (data not shown). Furthermore, treatment of cells with glucose oxidase facilitated the DNA damage caused by the addition of H_2O_2 bolus. This indicates

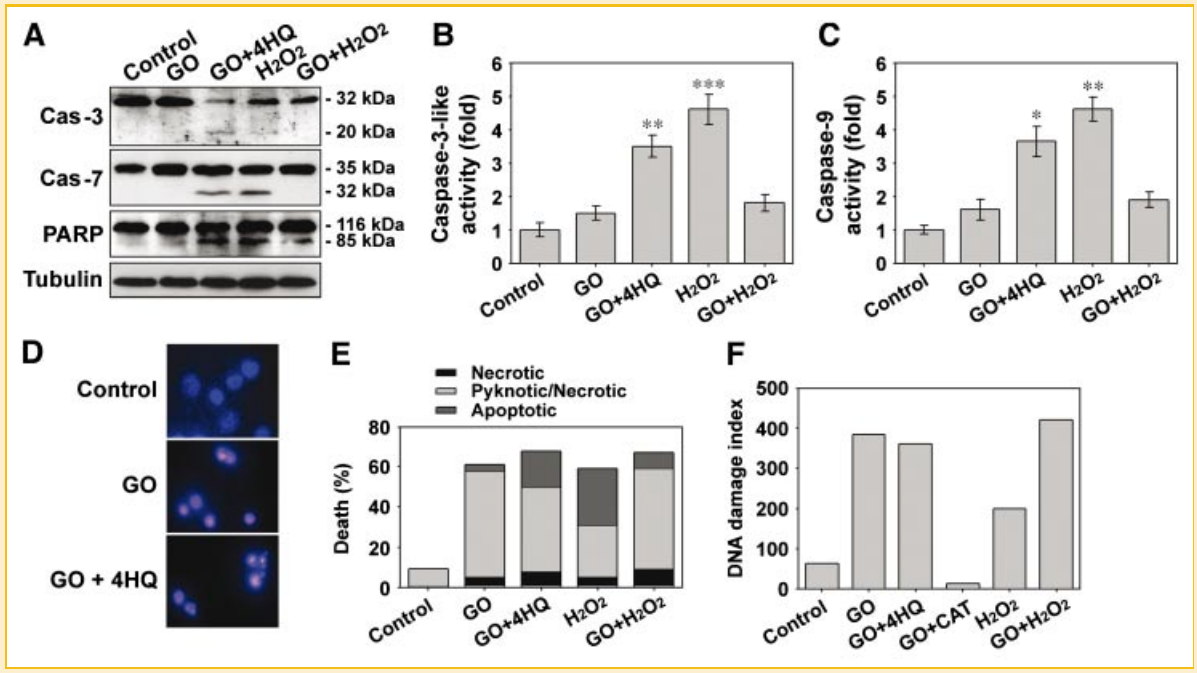

Fig. 5. PARP-1 inhibitor triggers caspase activation and subsequent nuclear fragmentation in glucose oxidase-treated cells. Cells were exposed to 10 mU/ml glucose oxidase, 200 μM H_2O_2 and/or 50 μM 4HQ for 12 h and protein extracts were prepared to analyze cleavage of caspase-3, caspase-7, and PARP by Western blotting (A) or to determine caspase-3-like (B) and caspase-9 activities (C). Cells were also treated with the same H_2O_2 exposure condition for 24 h and then stained with Hoechst 33342/PI without any fixation process. Photograph in (D) is representative data from triplicate experiments; the mode of cell death was morphologically classified into three types, as described in the Materials and Methods Section (E). F: In addition, cells exposed to the H_2O_2 generating system for 6 h were processed for comet assay. DNA damage index was calculated and represented in the same ways as described in Figure 1. [Color figure can be viewed in the online issue, which is available at www.interscience.wiley.com.]

that PARP-1 activation is downstream of the increased ROS generation after glucose oxidase treatment.

INHIBITION OF PARP-1 PREVENTS NUCLEAR TRANSLOCATION OF AIF AND ENDOG IN GLUCOSE OXIDASE-TREATED CELLS

To verify the precise role of PARP-1 on relocation of the death effector proteins, AIF and EndoG, the cells exposed to glucose oxidase and/or 4HQ were processed for Western blot analysis and immunostaining. PARP-1 inhibitor significantly prevented the H_2O_2-mediated nuclear translocation of AIF and EndoG from mitochondria (Fig. 6A,B). Confocal analysis revealed that these death effectors were mostly present in the nuclei of cells treated with 10 mU/ml glucose oxidase, whereas cells co-treated with 50 μM 4HQ showed localization in their mitochondria (Fig. 6C).

DISCUSSION

Intracellular ROS accumulation causes cell death by apoptosis, necrosis, or pyknosis. Numerous studies have shown that H_2O_2 by bolus addition induces apoptosis through caspase-dependent pathways, whereas the continuous presence of H_2O_2 inhibits the execution of the apoptotic process. It is a common phenomenon that apoptosis utilizing caspase cascades have energy-requiring steps and thus a persistent drop of ATP prevents caspase activation [Cregan et al., 2004; Kang et al., 2004; Sancho et al., 2006]. Our results show that continuously generated H_2O_2 but not bolus addition severely depletes the intracellular energy supply, which is closely associated with the prevention of apoptotic cell death caused by a bolus H_2O_2 addition. Although the mechanisms by which bolus versus continuous exposure to H_2O_2 has different effects in deciding the mode of cell death have been suggested [Barbouti et al., 2007; Son et al., 2009], here we further clarify that a low and continuous presence of H_2O_2 causes excessive DNA damage and PARP-1 activation, which signals rapid ATP depletion and relocation of AIF and EndoG, eventually leading to a caspase-independent cell death, mainly by pyknosis (Fig. 7).

There were many investigations emphasizing the important role of PARP-1 in the energy depletion and cell death modulation in H_2O_2-exposed cells [Szabó et al., 1996; Kang et al., 2004; Park et al., 2005]. However, the signaling molecules that mediate ATP depletion and subsequent pyknotic cell death in the continuous presence of H_2O_2 are not completely understood. The most important finding of this study is that PARP-1 also plays a role in this mediation. Here we verify that the PARP-1 activation in the continuous presence of H_2O_2 leads to at least two different downstream signals. One signal induces the almost complete drop of intracellular ATP levels and then mediates the inactivation of caspases. The other signal promotes MMP loss and nuclear translocation of AIF and EndoG from the mitochondria. Therefore, a prolonged or persistent activation of PARP-1 might cause a depletion of NAD^+ and cellular energy, eventually leading to pyknotic and/or necrotic cell death without the formation of a typical apoptotic body [Peralta-Leal et al., 2009]. Collectively, our results confirm the different roles of PARP-1 in deciding the mode of

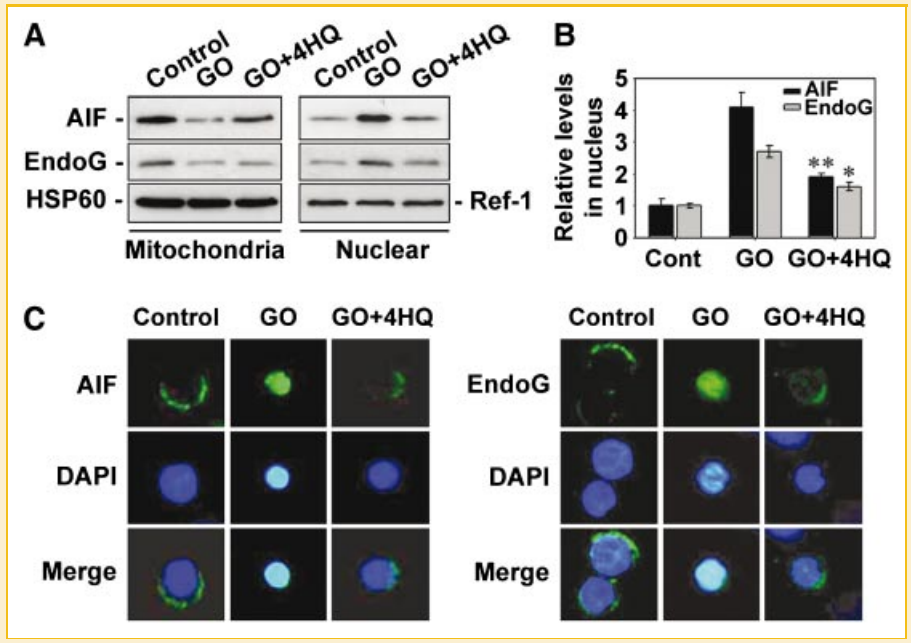

Fig. 6. Inhibition of PARP-1 blocks the nuclear translocation of AIF and EndoG in glucose oxidase-treated cells. Cells were subjected to 10 mU/ml glucose oxidase and/or 50 μM 4HQ for 12 h. A: Cell fractions were analyzed by 12% SDS–PAGE followed by immunoblotting against AIF and EndoG, and a representative result from triplicate experiments is shown. HSP60 and Ref-1 served as internal markers specific to mitochondrial and nuclear fractions, respectively. B: The relative levels of these death effectors in nuclear fractions were quantified, and $^{*}P < 0.05$ and $^{**}P < 0.01$ represent significant differences between the treatments with glucose oxidase/4HQ and glucose oxidase alone. C: Cells stained with FITC-AIF or FITC-EndoG were counterstained with DAPI. Confocal microscopic data shown are a representative result from three independent experiments and the overlay represents the fusion image of green (the effector proteins) and blue (nucleus). [Color figure can be viewed in the online issue, which is available at www.interscience.wiley.com.]

cell death according to the method of H_2O_2 generation, that is, by continuous generation versus a direct addition.

Key signaling molecules are tightly affected by the intracellular redox state. We previously found that exposure of cells to a continuously generated H_2O_2 but not bolus H_2O_2 leads to the prolonged and dramatic depletion of intracellular antioxidant defense systems, especially of thiol-containing antioxidant enzymes (data not shown). With this regard, we also postulated that continuously generated H_2O_2 diminished the activity of antioxidant enzymes, by which DNA damage and subsequent PARP activation were facilitated. This hypothesis can be supported by the current finding that the combined treatment with glucose oxidase and bolus H_2O_2 abolished apoptotic cell death, and that catalase almost completely inhibited H_2O_2-mediated DNA damage.

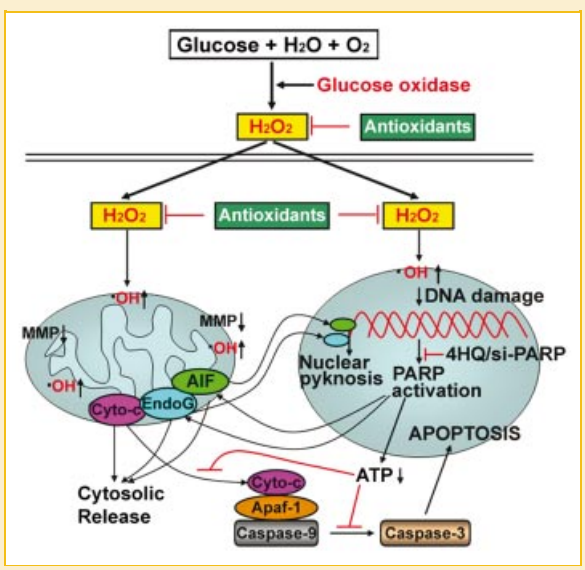

Fig. 7. Signaling pathways involved in PARP activation and caspase-independent pyknosis in cells exposed to chronic oxidative stress. [Color figure can be viewed in the online issue, which is available at www.interscience.wiley.com.]

On the other hand, mitochondria are key players in cell death, and an important mitochondrial event during cell death is the loss of MMP [Kowaltowski et al., 2001; Kim et al., 2003]. MMP loss is induced by organelle swelling and membrane rupture or by the action of Bcl-2 family proteins, such as Bcl-2 and Bax [Epand et al., 2002]. We have previously shown that continuously generated H_2O_2 results in the decrease of Bcl-2 and the increase of Bax [Son et al., 2009]. Although the mechanisms of the Bcl-2 family on H_2O_2-mediated mitochondrial stress are unclear at present, these proteins might participate in H_2O_2-mediated changes of mitochondrial events. Furthermore, activation of caspase cascades and nuclear translocation of mitochondrial death effectors are not the sole determinant of a cell's destiny. It would be worthwhile to investigate the exact functional relationship between PARP-1 and Bcl-2 proteins or Bcl-2 proteins and mitochondrial stress under both H_2O_2 systems.

Other interesting finding in this investigation was that the role of PARP-1 in deciding the mode of cell death depends closely on the

timing of H_2O_2 exposure rather than the H_2O_2 concentration employed. It is possible that when an H_2O_2 bolus is added to cells it rapidly diffuses [Barbouti et al., 2002], whereas glucose oxidase produces H_2O_2 at relatively low and continuous way for at least 24 h after treatment [Lee et al., 2006]. The latter case is similar to the conditions of in vivo H_2O_2 generation [Chance et al., 1979]. Furthermore, the inhibition of H_2O_2-induced cell death by blocking PARP-1 is temporary, whereas catalase prevented mainly DNA damage and H_2O_2-mediated cell death. This could mean that PARP-1 has a partial role in cell death caused under a condition of prolonged and persistent oxidative stress.

In summary, accumulating evidence has implicated that PARP is a target for therapeutic intervention in critical illness because the inhibition of PARP activity is thought to have a protection against a variety of inflammatory diseases [Peralta-Leal et al., 2009]. However, our results indicate that antioxidant application rather than molecular targeting to regulate a death effector or step involved in H_2O_2-mediated cell death might prove more useful for protection against oxidant-mediated degenerative diseases. Overall, the importance of understanding the cellular events and changes in H_2O_2-exposed cells under similar in vivo conditions should be taken into consideration.

REFERENCES

Barbouti A, Doulias PT, Nousis L, Tenopoulou M, Galaris D. 2002. DNA damage and apoptosis in hydrogen peroxide-exposed Jurkat cells: Bolus addition versus continuous generation of H_2O_2. Free Radic Biol Med 33:691–702.

Barbouti A, Amorgianiotis C, Kolettas E, Kanavaros P, Galaris D. 2007. Hydrogen peroxide inhibits caspase-dependent apoptosis by inactivating procaspase-9 in an iron-dependent manner. Free Radic Biol Med 43:1377–1387.

Bernstein C, Bernstein H, Payne CM, Garewal H. 2002. DNA repair/pro-apoptotic dual-role proteins in five major DNA repair pathways: Fail-safe protection against carcinogenesis. Mutat Res 511:145–178.

Bradford MM. 1976. A rapid and sensitive method for the quantitation of microgram quantities of protein utilizing the principle of protein-dye binding. Anal Biochem 72:248–254.

Chance B, Sies H, Boveris A. 1979. Hydroperoxide metabolism in mammalian organs. Physiol Rev 59:527–605.

Comelli M, Genero N, Mavelli I. 2009. Caspase-independent apoptosis in Friend's erythroleukemia cells: Role of mitochondrial ATP synthesis impairment in relocation of apoptosis-inducing factor and endonuclease G. J Bioenerg Biomembr 41:49–59.

Cregan SP, Dawson VL, Slack RS. 2004. Role of AIF in caspase-dependent and caspase-independent cell death. Oncogene 23:2785–2796.

Epand RF, Martinou JC, Montessuit S, Epand RM, Yip CM. 2002. Direct evidence for membrane pore formation by the apoptotic protein Bax. Biochem Biophys Res Commun 298:744–749.

Erdélyi K, Bakondi E, Gergely P, Szabó C, Virág L. 2005. Pathophysiologic role of oxidative stress-induced poly(ADP-ribose) polymerase-1 activation: Focus on cell death and transcriptional regulation. Cell Mol Life Sci 62:751–759.

Kang YH, Yi MJ, Kim MJ, Park MT, Bae S, Kang CM, Cho CK, Park IC, Park MJ, Rhee CH, Hong SI, Chung HY, Lee YS, Lee SJ. 2004. Caspase-independent cell death by arsenic trioxide in human cervical cancer cells: Reactive oxygen species-mediated poly(ADP-ribose) polymerase-1 activation signals apoptosis-inducing factor release from mitochondria. Cancer Res 64:8960–8967.

Kim JS, He L, Lemasters JJ. 2003. Mitochondrial permeability transition: A common pathway to necrosis and apoptosis. Biochem Biophys Res Commun 304:463–470.

Kowaltowski AJ, Castilho RF, Vercesi AE. 2001. Mitochondrial permeability transition and oxidative stress. FEBS Lett 495:12–15.

Lee JC, Son YO, Choi KC, Jang YS. 2006. Hydrogen peroxide induces apoptosis of BJAB cells due to formation of hydroxyl radicals via intracellular iron-mediated Fenton chemistry in glucose oxidase-mediated oxidative stress. Mol Cells 22:21–29.

Li GY, Osborne NN. 2008. Oxidative-induced apoptosis to an immortalized ganglion cell line is caspase independent but involves the activation of poly (ADP-ribose) polymerase and apoptosis-inducing factor. Brain Res 1188:35–43.

Lin T, Yang MS. 2008. Benzo(α)pyrene-induced necrosis in the HepG(2) cells via PARP-1 activation and NAD(+) depletion. Toxicology 245:147–153.

Martin D, Salinas M, Fujita N, Tsuruo T, Cuadrado A. 2002. Ceramide and reactive oxygen species generated by H_2O_2 induce caspase-3-independent degradation of Akt/protein kinase B. J Biol Chem 277:42943–42952.

Maulik N, Sato M, Price BD, Das DK. 1998. An essential role of NF-kappaB in tyrosine kinase signaling of p38 MAP kinase regulation of myocardial adaptation to ischemia. FEBS Lett 429:365–369.

Panayiotidis M, Tsolas O, Calaris D. 1999. Glucose oxidase-produced H_2O_2 induces Ca^{2+}—dependent DNA damage in human peripheral blood lymphocytes. Free Radic Biol Med 26:548–556.

Park MT, Kim MJ, Kang YH, Choi SY, Lee JH, Choi JA, Kang CM, Cho CK, Kang SK, Bae S, Lee YS, Chung HY, Lee SJ. 2005. Phytosphingosine in combination with ionizing radiation enhances apoptotic cell death in radiation-resistant cancer cells through ROS-dependent and -independent AIF release. Blood 105:1724–1733.

Peralta-Leal A, Rodríguez-Vargas JM, Aguilar-Quesada R, Rodríguez MI, Linares JL, de Almodóvar MR, Oliver FJ. 2009. PARP inhibitors: New partners in the therapy of cancer and inflammatory diseases. Free Radic Biol Med 47:13–26.

Sancho P, Fernández C, Yuste VJ, Amran D, Ramos AM, de Blas E, Susin SA, Aller P. 2006. Regulation of apoptosis/necrosis execution in cadmium-treated human promonocytic cells under different forms of oxidative stress. Apoptosis 11:673–686.

Son YO, Jang YS, Heo JS, Chung WT, Choi KC, Lee JC. 2009. Apoptosis-inducing factor plays a critical role in caspase-independent, pyknotic cell death in hydrogen peroxide-exposed cells. Apoptosis 14:796–808.

Szabó C, Zingarelli B, O'Connor M, Salzman AL. 1996. DNA strand breakage, activation of poly (ADP-ribose) synthetase, and cellular energy depletion are involved in the cytotoxicity of macrophages and smooth muscle cells exposed to peroxynitrite. Proc Natl Acad Sci USA 93:1753–1758.